Enhanced Protective Properties and Structural Order of SelfAssembled Monolayers of Aromatic Thiols on Copper in Contact with Acidic Aqueous Solution

ARTICLE *in* THE JOURNAL OF PHYSICAL CHEMISTRY C · FEBRUARY 2012

Impact Factor: 4.77 · DOI: 10.1021/jp210041v

THE JOURNAL OF PHYSICAL CHEMISTRY C

Article

pubs.acs.org/JPCC

Enhanced Protective Properties and Structural Order of Self-Assembled Monolayers of Aromatic Thiols on Copper in Contact with Acidic Aqueous Solution

Fabrizio Caprioli,* Andrea Martinelli, Delia Gazzoli, Valeria Di Castro, and Franco Decker

Dipartimento di Chimica, Università "Sapienza", Piazzale le Aldo Moro 5, 00185, Rome, Italy

Supporting Information

ABSTRACT: In the present work we used different techniques to study self-assembled monolayers (SAMs) of two aromatic thiols, namely, benzenethiol (BT) and 2-naphthalenethiol (2-NT), and one alkylic thiol, 1-undecanethiol (1-UT), on polycrystalline copper, comparing their corrosion inhibition efficiency and their stability up to a week in H_2SO_4 0.5 M. Both electrochemical impedance spectroscopy (EIS) and linear polarization highlighted different aging trends for 1-UT on one side and aromatic thiols on the other. 1-UT was initially the best corrosion inhibitor among the three thiols, as expected from its larger thickness, but it degraded very rapidly. On the contrary, BT and 2-NT showed a noticeable increase of their protective properties during the first hours of exposure to the electrolyte leading to a superior performance over any 1-UT sample. Raman spectroscopy suggested this behavior to be related to an enhancement of the structural order of the aromatic layer. In addition, both XP spectroscopy and electrochemical measurements revealed BT and 2-NT layers to be stabler than 1-UT. In particular, BT layers exposed to H_2SO_4 0.5 M exhibited better protective properties, with respect to the freshly prepared samples, lasting for over 1 week of aging.

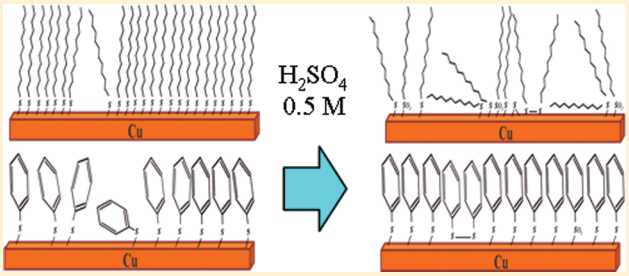

INTRODUCTION

Thanks to its favorable thermal, mechanical, and electric properties,[1] copper is today an irreplaceable material in many fields: from electrical engineering to buildings to computer and integrated circuit manufacture, where it is increasingly replacing aluminum owing to its larger electrical conductivity and heat dissipation capacity. Unfortunately copper is subject to corrosion when exposed to air or to other oxidizing environments, seriously affecting its performance in most of its applications and making necessary the protection of the surface by organic coatings.

Since Laibinis and Whitesides demonstrated that *n*-alkanethiolates are able to self-assemble on a copper surface[2] protecting it from air oxidation,[3] the effectiveness of self-assembled monolayers (SAMs) as corrosion inhibitors has been the object of several studies, which have shown how these systems provide excellent performance either in acidic,[4−6] alkaline,[7−10] closely neutral,[11−15] or chloride containing solutions.[7−10,16,17] This is due to the high stability of the S−Cu bond, considerably stronger than the corresponding S−Au bond,[18,19] and to the close-packed structure of the SAMs, acting as a barrier against oxidizing molecules. In fact, the superiority of 1-dodecanethiol over benzotriazole, the most widely used corrosion inhibitor for copper, has been recently demonstrated in various environments.[10,11,20] The direct relationship, observed for the *n*-alkanethiolates, between the layer thickness and the protective properties of the SAMs[14,21] boosted the investigations, until today, of long chain alkylic thiols[3−6,10−17,21] ($CH_3-(CH_2)_n-SH$ with $n \geq 10$) and of their synthetically favorable derivates allowing the formation of a relatively thick (3−6 nm) protective film. For example, the modification of 11-mercapto-1-undecanol SAMs with alkylchlorosilanes has been extensively studied by Aramaki et al.,[22−27] whereas more recently Laibinis et al. tested the efficiency of long chain *ω*-alkoxy-*n*-alkanethiols.[28,29] Very few studies, on the other hand, have been performed on the shorter aromatic thiols,[30−34] although Zamborini et al. had already observed that these molecules provide a better protection against the corrosion of under-potential deposited (UPD) copper than alkanethiols of comparable length.[34] In fact, in contrast with benzenethiol (BT) monolayers on gold surfaces, having a poorly defined structure characterized by sparse molecules with a large tilt angle (∼ 50°),[35,36] BT SAMs on copper surfaces are expected to be densely packed and in upright configuration, with a tilt angle of approximately 20°.[37,38]

In a recent work[32] we studied the behavior of three different SAMs of aromatic thiols immersed in a strong acidic solution for 12 hours. An unexpected electrochemical response of the aromatic SAMs was observed with a noticeable increase in the charge−transfer resistance within the first few hours of immersion. The SAMs of alkylic thiols, on the contrary, are

Received: October 19, 2011
Revised: January 26, 2012
Published: January 27, 2012

   dx.doi.org/10.1021/jp210041v | J. Phys. Chem. C 2012, 116, 4628−4636

known to undergo a fast degradation in their inhibition properties when exposed to aggressive solutions.[5,6]

In order to more deeply investigate the reasons of these opposite trends as corrosion inhibitors of the aromatic versus the alkylic thiols, we proceeded as follows. Two simple aromatic thiols, namely, BT and 2-naphthalenethiol (2-NT), and one alkylic thiol, the 1-undecanethiol (1-UT), have been chosen to form protective SAMs on polycrystalline Cu electrodes with a similar adsorption protocol. Geometrical calculation performed using bond lengths and tilt angles reported in the literature[21,38,39] revealed that the selected molecules form monolayers with remarkably different thickness (around 0.65 nm for BT, 0.90 for 2-NT, and 1.60 for 1-UT). The stability and the electrochemical passivity of such modified electrodes upon immersion in H_2SO_4 0.5 M for up to 1 week have been followed by two different electrochemical techniques, namely, electrochemical impedance spectroscopy (EIS) and linear polarization. In addition, dynamic contact angle analysis (DCA) and Raman spectroscopy have been repeatedly applied to both freshly prepared and aged samples to obtain information on the hydrophobicity and on the molecular structure of the SAM on the Cu electrode, as a function of the immersion time. At the same time, X-ray photoelectron spectroscopy (XPS) has been systematically performed on both fresh and aged samples in order to assess the surface composition, the presence of contaminants and/or of copper oxides, as well as the stability of the S−Cu and S−C bond in the molecular layers. The purpose of this work is to test the actual stability and efficiency of aromatic SAMs, which, by our preliminary data,[40] seem to be higher compared to the traditional layers of *n*-alkanethiolate in spite of the lower thickness, and possibly determine the causes of their interesting behavior. This assumes importance considering that the employment of SAMs, not only as copper corrosion inhibitors, is still today mainly curbed by their limited durability.[41]

EXPERIMENTAL SECTION

Sample Preparation. The SAMs deposition was performed using as substrates plates of pure (99.95%) polycrystalline copper, commercially available from Goodfellows, Ltd. In order to prepare a clean Cu surface to the thiol adsorption, a multistep polishing procedure was followed: the samples were initially physically polished by abrasive paper and then kept for 15 min in an ultrasonic bath in acetone, to remove possible organic impurities. Subsequently, the plates were etched for 30 s in concentrated HNO_3 (32.5%), rapidly rinsed with distilled water, further etched for 7 min in diluted HCl (3.7%), and finally copiously rinsed with distilled water, obtaining a fresh, reactive, and oxide-free surface. The samples used as standard copper were dried under nitrogen flow and immediately characterized. The adsorption of the monolayers was carried out by 24 h of immersion of the polished substrate in a 0.75 mM solution of the suitable thiol, obtained from direct dissolution of BT (≥99%, Sigma-Aldrich), 2-NT (99%, Acros Organics) and 1-UT (98%, Sigma-Aldrich) in technical ethanol (96% Carlo Erba reagents). Differently from our previous studies on these systems,[32,33] we adopted a lower thiol concentration and a longer exposition time to the solution in order to obtain the highest surface coverage and the best molecular order for the monolayers, and to minimize the presence of physisorbed material at the same time. After 24 h, the samples were copiously rinsed with ethanol, dried under nitrogen flow, and immediately characterized.

XPS Measurements. XPS measurements were performed using a modified Omicron MXPS system with a dual anode X-ray source (Omicron DAR 400) and an Omicron EA-125 energy analyzer, using Mg K_α photons ($h\nu$ = 1253.6 eV) generated operating the anode at 14−15 kV, 10−20 mA. All the reported XP spectra were acquired using an analyzer pass energy of 20 eV and a takeoff angle of 11° with respect to the surface normal. All the measurements were carried out at room temperature with a pressure in the analyzer chamber lower than 2×10^{-9} mbar during the spectra detection. No sign of sample degradation or charging effects, such as broadening or progressive shift, under the X-rays were observed during acquisition times (about 1 h for each sample). The binding energy of the Cu $2p_{3/2}$ line at 932.7 eV was used as the internal standard reference. The experimental spectra were theoretically reconstructed by fitting with symmetric Voigt functions with a Gaussian−Lorentzian ratio allowed to vary between 50% and 100%. To quantify the adlayer atomic composition, XPS atomic ratios were estimated from experimentally determined area ratios of the relevant core lines corrected for the corresponding Scofield cross sections.[42] For all the SAMs, measurements were carried out both on freshly prepared samples and after different times of immersion in the acidic solution (6, 24, 48, 72, 120, and 170 h). Before each experiment, aged plates were copiously rinsed with ultrapure water and dried under nitrogen flow.

Electrochemical Measurements. The electrochemical experiments were performed using a conventional three electrode cell, where the counter electrode was a platinum wire and the reference electrode was an Ag/AgCl/Sat. KCl electrode (+0.197 V vs SHE). All the reported potentials in this paper are referred to this value. A flat copper working electrode was pressed against an O-ring, sealing a small aperture opened in the lateral wall of the cell, defining exactly the electrode area (0.33 cm^2). All measurements were performed at room temperature (24 ± 1 °C) and in an aerated 0.5 M H_2SO_4 solution as electrolyte. The instrumentation consisted of a computer-controlled Autolab Electrochemical Analyzer (model PGSTAT 12, Eco Chemie BV, The Netherlands), whereas the acquisition programs were GPES and FRA version 4.6. The EIS spectra were recorded at the open circuit potential (OCP) in a frequency range between 30 kHz and 50 mHz, with a modulation amplitude of 0.01 V. To extrapolate the parameters of the equivalent circuit, the data were fitted using ZSimpwin 3.21 software. The linear polarization measurements were carried out in anodic direction starting from −0.3 V up to +0.3 V, at a scan rate of 1 mV s^{-1}, and the data were analyzed by GPES version 4.6, allowing the calculation of the exchange current.

DCA Measurements. DCA measurements were carried out by employing a dynamic contact angle analyzer (DCA-322, Chan, CA) based on the tensiometric Wilhelmy method. The advancing (ϑ_{adv}) and receding (ϑ_{rec}) contact angles were recorded by immersing and withdrawing the sample in deionized water (Water Plus, Carlo Erba, gw = 72.6 mN m^{-1}) at a stage speed of 100 $\mu m \cdot s^{-1}$.

After the aging in 0.5 M H_2SO_4 water solution for a predetermine period of time, the SAM samples were copiously rinsed with ultrapure water, dried under nitrogen flow, and immediately analyzed.

Raman Spectroscopy. Raman spectra were collected in the backscattering geometry with an inVia Renishaw spectrometer equipped with an air-cooled CCD detector and a super-Notch filter. The 785.0 nm emission line from a diode

dx.doi.org/10.1021/jp210041v | J. Phys. Chem. C 2012, 116, 4628−4636

laser was focused on the sample under a Leica DLML microscope using a 20x objective. The spectral resolution was 2 cm^{-1}, and the spectra were calibrated using the 520.5 cm^{-1} line of a silicon wafer. Repeated (10−20) 10 s scans were accumulated for each experimental run to provide better signal-to-noise ratios with a power of the incident beam on the sample of about 5 mW. Multiple spot analyses were carried out on different regions of the same sample to check for spectral reproducibility. Data analysis included baseline removal and curve fitting using a Gauss-Lorentz cross-product function by Peakfit 4.12 software (Jandel, AISN Software).

RESULTS

Electrochemical Characterization. The equivalent circuit adopted to fit the EIS data for protected copper is shown in Figure 1. This model, previously described elsewhere,[32] has

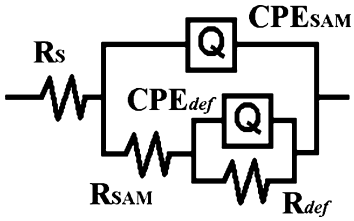

Figure 1. Equivalent circuit employed to analyze EIS data relative to coated Cu electrodes.

been proposed by several authors to describe the behavior of SAMs containing defects when the mass transport contribution may be neglected.[6,17,43−45] In order to evaluate the properties of the various SAMs, three parameters were considered: (i) the overall charge-transfer resistance R_{tot}, being the sum of R_{SAM} and R_{def}, (ii) the open circuit (or corrosion) potential (OCP), and (iii) the frequency independent parameter Y_0 associated with the constant phase element CPE_{SAM}. Y_0 has been considered a representative of the SAM capacitance since in our experiments n_{SAM} was always found to be higher than 0.9.

The measurements performed on the freshly prepared samples show that the charge transfer resistance at $t = 0$ scaled up with the thickness of the monolayers (Figure 2a). Even if BT provided a good protection of the underlying copper, the EIS data clearly show that the resistance of the thicker 2-NT was roughly twice, and that of 1-UT even much larger than, that of BT. The freshly prepared 1-UT SAM presented in fact excellent protective properties, with an R_{tot} around 15 kΩ cm^2, i.e., more than 2 orders of magnitude higher than that of uncoated copper. Nevertheless, in the course of exposure of the 1-UT samples to acidic solution, their charge-transfer resistance became half of the initial value already after 6 h, and further decreasing to 20% after 24 h, and to 5% after one week. This dramatic loss in the inhibition efficiency of long-chain alkylic SAMs subsequent to their exposure to an aggressive environment has been already described by various authors.[5,6,28] The SAMs of aromatic thiols showed the opposite trend in the first hours of immersion in acid, namely, a steep increase in their charge-transfer resistance, reaching values exceeding that of the freshly prepared 1-UT. This behavior of BT and 2-NT went along with a clear shift of their OCP in the negative direction (from ca. −10 mV to ca. −70 mV, Figure 2b), suggesting the growth of their protective properties to be mainly related to the inhibition of the cathodic reaction, i.e., the reduction of dissolved oxygen.

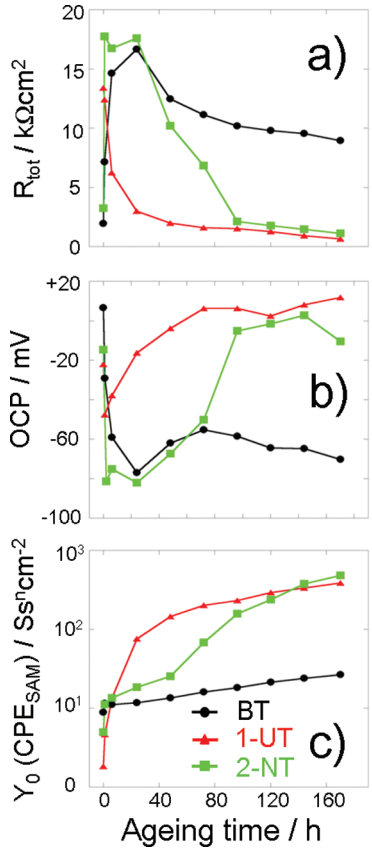

Figure 2. Evolution of the circuit parameters, extracted by fitting EIS data, as a function of the aging time for various samples: −●− BT, −▲− 1-UT, and −■− 2-NT. (a) Evolution of the total charge transfer resistance $R_{tot} = R_{SAM} + R_{def}$. (b) Evolution of the OCP. (c) Evolution of the frequency-independent parameter Y_0 associated with CPE_{SAM}.

Regarding the aromatic SAM durability, Figure 2a,b shows that after two or three days in these aging conditions, 2-NT underwent a sudden breakdown, with a collapse of the overall charge-transfer resistance accompanied by a concomitant increase of the OCP. After aging for about 100 h, there was almost no difference in the performance of 1-UT and 2-NT, with respect to charge-transfer resistance and to OCP. BT SAMs showed, on the contrary, a much longer durability: their performance reached a maximum during the first 24 h of aging, and then decreased slightly and linearly. Yet after one week, its inhibition efficiency was still clearly higher than that of freshly prepared samples, as highlighted by the EIS parameters (R_{tot}, CPE_{SAM}) and OCP.

The capacitance of all the modified electrodes, extracted from the fitting of EIS data, increased with time, although with different slopes (Figure 2c). Because SAMs can be assimilated to dielectric within planar capacitors,[21] the increasing trend can be attributed to the formation of defects and/or collapsed sites during immersion, allowing the penetration of electrolyte in the SAM, with increase of its relative permittivity and decrease of the average layer thickness. The steepest increase in electrode capacitance has been detected for 1-UT confirming the rapid degradation of this sample in acidic electrolyte. The lowest slope in the plots in Figure 2c is that of the BT-coated electrode, that appears to be the most stable among the three samples. The electrode capacitance for the 2-NT-coated sample was close to that of BT in the first part of the experiment, but gradually increased and approached the same values as for the

dx.doi.org/10.1021/jp210041v | J. Phys. Chem. C 2012, 116, 4628−4636

1-UT electrode after 100 h aging, with a similar behavior to that already observed for its OCP and its charge-transfer resistance.

The trend shown by EIS experiments was also confirmed by linear polarization measurements, illustrated in the Tafel plots (Figure 3a,b,c). There was a clear inhibition effect by the three

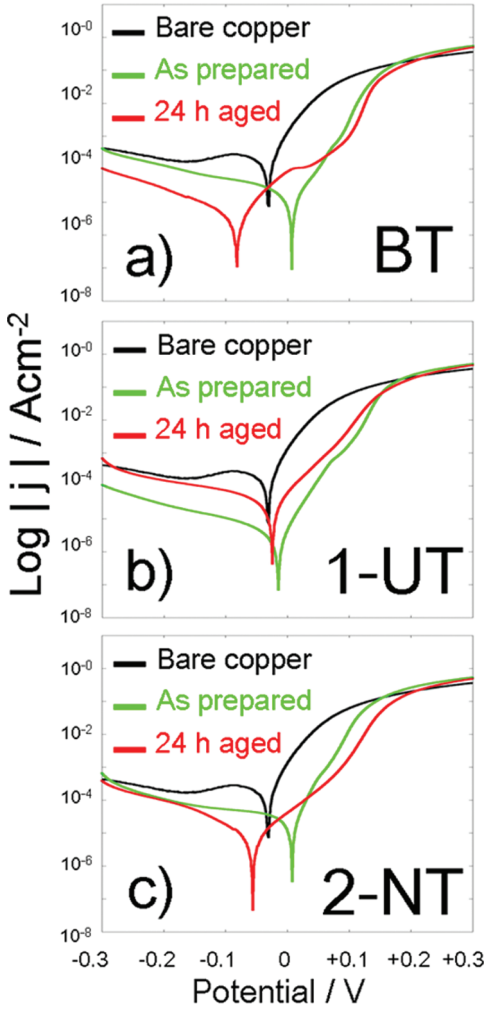

Figure 3. Linear polarization curve, recorded in the anodic direction at a scan rate of 1 mV s^{-1}, relative to (green line) freshly prepared and (red line) 24 h aged samples of (a) BT, (b) 1-UT, and (c) 2-NT. A curve relative to freshly cleaned Cu bare (black line) has been included for comparison.

SAMs, in comparison with the Tafel plot of a naked Cu electrode. In such plots and, namely, in the negative potential region, the passivation effect was progressive with exposure time only for the aromatic SAMs. The 1-UT layer, on the contrary, allowed a very good inhibition at first, but had a short lasting effect as evidenced in all Tafel plots recorded on previously aged samples. The extrapolation of the corrosion current clearly shows primarily that all the freshly prepared samples ensure a good protection to the underlying substrate, with a decrease of more than 1 order of magnitude with respect to the value obtained for the uncoated copper. The inhibition efficiency initially followed the order 1-UT > 2-NT > BT, accordingly with the layer thickness and in agreement with the impedance data. Nevertheless, after 24 h aging, both the SAMs of aromatic thiols showed an evident decrease of the corrosion current and a negative shift (by ~70 mV) of the corrosion potential. The inhibition properties by the aged BT and 2-NT in this instance approached those of the freshly prepared 1-UT, which, on the other hand, recorded a dramatic increase in its corrosion current, thus confirming the fast layer degradation previously detected with EIS measurements.

XPS Measurements. XPS was used to characterize both freshly prepared and aged samples. The analysis of the S 2p region of the as-prepared samples reveals the presence of a main doublet (1.2 eV shift, 2:1 ratio) with a maximum at 162.3 ± 0.1 eV, assigned to the Cu−S thiolate bond.[7,30,40] In the case of BT and 1-UT, no other components were observed, indicating the absence of a detectable quantity of physisorbed molecules or oxidation products. On the contrary, the spectrum of 2-NT showed two minor components, with a maximum at 163.4 ± 0.1 eV and 167.7 ± 0.2 eV, which were ascribed to physisorbed material[46,47] and traces of sulfonates.[2,47] Nevertheless, the main component due to the chemisorbed thiolate, represented around the 95% of the total sulfur also in the 2-NT. Moreover, the high values of the S/Cu ratio (0.50 for BT, 0.55 for1-UT, 0.57 for 2-NT) suggested for all the samples a good coverage of the copper substrate.[48]

The main C1s signals were found at 284.1 ± 0.1 eV and 285.0 ± 0.1 eV for aromatic and alkylic thiols, respectively, accordingly to the literature.[49,50] These peaks are enlarged by a minor component at slightly higher binding energy (around 0.6−0.7 eV) ascribed to the carbon atom bonded to the sulfur. The shape of the peaks and the experimental C/S atomic ratios (5.7 for BT, 11.7 for 1-UT, and 9.7 for 2-NT) demonstrate the absence of a significant amount of organic impurities, while the Cu 2p XP spectra (available in the Supporting Information) excluded the presence of Cu(II) for all the samples.

The measurements carried out on samples aged in acidic solution for different times (6, 24, 48, 72, 120, and 170 h) allowed us to check the evolution of the adsorbed layer. The trend of the S/Cu ratio, (after a week, 0.66 for BT, 0.70 for 1-UT, and 0.92 for 2-NT) confirmed that in all the samples the thiols resist the copper surface even in these aggressive conditions. The slight increase observed is probably related to a weakening of the Cu $2p_{3/2}$ signal, which was used in the calculation of the atomic ratio, due to the absorption of impurities and/or to a partial oxidation of the surface following the aging process. The presence of contaminants on the surface was also confirmed by the progressive increase of the C/S ratio (after a week, 9.6 for BT, 16.3 for 1-UT, and 18.0 for 2-NT). The increase of the oxygen content in the aged samples, on the other hand, can be attributed to several causes: the formation of copper oxide, the adsorption of adventitious organic contaminants, the oxidation of some thiols to sulfonate, and the presence of some electrolyte molecules trapped in the layer or adsorbed on the metal surface. So, following the oxygen abundance on a sample allows one to roughly estimate its permeability to the electrolyte and its tendency toward oxidation. The O/S ratios, reported in Figure 4b, actually showed a growing trend for all the samples. Nevertheless, the BT samples constantly showed values considerably smaller than those of 2-NT and 1-UT, suggesting that this SAM is the less permeable layer and the less prone to oxidation, thus the most effective in the substrate protection, in spite of its lower thickness. Moreover, the fits carried out on the S 2p spectra relative to aged samples are consistent with these surprising results, showing a noticeable difference of stability between the SAMs of aromatic thiols and the 1-UT samples. In fact, as shown in Figure 4a, even after several days in 0.5 M H_2SO_4, the

dx.doi.org/10.1021/jp210041v | J. Phys. Chem. C 2012, 116, 4628−4636

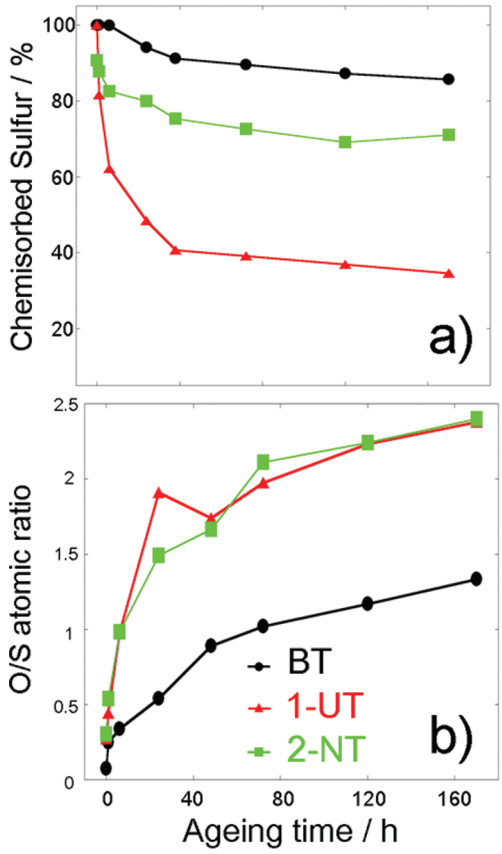

Figure 4. Evolution of atomic ratios, extracted by XPS data, as a function of the aging time for various samples: −●− BT, −▲− 1-UT, and −■− 2-NT. (a) Evolution of the ratio between chemisorbed thiolate sulfur and total detected sulfur; (b) evolution of the ratio between total oxygen and total sulfur.

majority of the aromatic thiols remained steadily chemisorbed to the copper surface. SAMs made of BT proved to be extremely stable, so that even after 1 week of aging the component of the S 2p spectra ascribable to the sulfur covalently bonded to the substrate (162.3 ± 0.1 eV) represented around 85% of the total. The remaining signal was quite equally distributed between two minor components at 163.4 ± 0.1 eV and 167.7 ± 0.2 eV, assigned to traces of disulfide and sulfonates, respectively. Although they appeared less stable than BT, 2-NT samples showed a good durability in the aging condition as well. The fits of the S 2p peaks highlighted that, after 7 days, around 70% of molecules were still covalently bonded to the surface, whereas the percentage of both disulfide and sulfonates was roughly twice that observed for BT. 1-UT SAMs, on the contrary, seemed to undergo serious damage after a few hours of exposure to the acidic solution already. In fact after only 24 h aging in H_2SO_4, the percentage of chemisorbed thiol becomes less than 50% and as low as 35% after a week. Furthermore, in addition to the peaks at 163.4 ± 0.1 eV and 167.7 ± 0.2 eV, a new large component, lying at 161.6 ± 0.1 eV, appeared in the S 2p spectra relative to the aged 1-UT samples. This signal, indicative of the presence of Cu_2S on the surface,[51] demonstrates that under these aggressive conditions the S−C bonds in the alkylic SAMs are prone to breakage. This phenomenon, which we never observed with BT and 2-NT monolayers, is consistent with the significant difference in the S−C bond strength of alkylic and aromatic thiols (~86 kcal mol^{-1} for BT vs ~73 kcal mol^{-1} for *n*-alkylic thiols) reported in the literature.[52,53] It is worth noting that the great number of damaged molecules in aged 1-UT samples deduced by XP spectra is in very good agreement with electrochemical data, highlighting the dramatic instability of the alkylic layer leading to a loss in protective properties.

Raman Spectroscopy. Raman spectroscopy, in ordinary and surface-enhanced Raman scattering (SERS) detection setup, can provide convenient tools for investigating the molecular structure and the properties of aliphatic and aromatic thiols in terms of interaction, preferential orientation, and conformation.[54−59]

For our systems adsorbed on copper, the use of the 785 nm laser line in ordinary Raman setup is expected to yield an enhancement of the molecular layer very close to the metal surface.[54] Theoretical calculations predict three groups of bands for neat aromatic thiols, associated with metal−S stretching vibrations, displacement of the S atom within the ring, and benzene ring vibrations.[55] The most prominent benzene ring vibrations (υ12, υ18a, υ1, and υ8a C−C modes) occur at 1000, 1021, 1064, and 1572 cm^{-1} respectively, whereas bands appearing at 417, 701, 917, and 2561 cm^{-1} are assigned to the ν_{7a} and ν_{6a} ring modes with contributions from the C−S stretching vibration (νCS), the CSH deformation (δCSH) and the S−H stretching (νSH), respectively.

The measured spectrum of BT freshly adsorbed on copper (Figure 5a; red curve) showed distinct bands at about 406, 993,

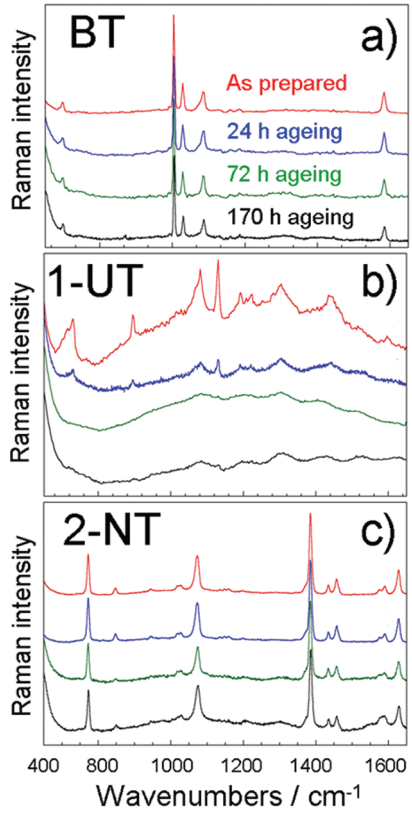

Figure 5. Raman spectra of (a) BT, (b) 1-UT, and (c) 2-NT on Cu in the region 650−1650 cm^{-1} as a function of aging time. (red line) freshly prepared sample; (blue line) after 24 h aging; (green line) after 72 h; (black line) after 170 h aging. Spectra are scaled and shifted for clarity.

dx.doi.org/10.1021/jp210041v | J. Phys. Chem. C 2012, 116, 4628−4636

1015, 1074, and 1574 cm^{-1} and a broad feature containing contribution at about 486, 534, 581, 612, 695 cm^{-1}. The first set of bands corresponds to C−H out-of-plane bending and C−S stretching, ring out-of-plane deformation, ring in-plane deformation, and C−C symmetric stretching with C−S contribution, respectively.[54,55,58] Further bands in the range 480−590 cm^{-1}, not shown in the plots, can result from the superimposition of C−S out-of-plane bending and vibrations from the CuO surface layer, whereas the band at about 612 and 695 cm^{-1} can be attributed to the ring in-plane deformation with contributions from the C−S stretching vibrations (νCS). The ν(Cu−S) stretching vibration is expected in the range 200−280 cm^{-1}, a region not clearly seen in our experimental set up. The absence of the S−H stretching mode (νS−H) at about 2586 cm^{-1} and of the S−H in-plane bending at about 915 cm^{-1} and the lowering in the band positions with respect to those of nonadsorbed BT molecules clearly indicate that BT adsorbed dissociatively as benzenethiolate, forming a copper−sulfur bond.[58] The temporal evolution of BT adsorbed on Cu (Figure 5a; blue, green, and black curves) could not prove any specific changes both in the relative peak intensities and in the position for the bands at about 993, 1015, 1074, and 1574 cm^{-1} with aging. Conversely, a progressive increase of oxide components on the copper surface was detected in the spectral range 400−800 cm^{-1}. The constancy in the relative intensity could, however, indicate that the orientation of BT molecules with respect to the surface remained practically unchanged, although no direct information on the orientation of the chemisorbed molecules can be extracted from our spectra.

In a dedicated experiment, some selected surface spots were sampled as a function of time, all the other parameters being constant, in order to avoid effects due to the inhomogeneity of the samples. Comparing the Raman spectra of freshly prepared and 24 h aged BT samples, a systematic increase in absolute Raman intensity was observed (Figure 6a). Although absolute Raman intensities are difficult to quantify because of their dependence on experimental conditions, this behavior seems indicative of a more regular surface morphology, accordingly with the electrochemical data.

The measured spectra of 2-NT adsorbed on copper (Figure 5c, red curve) show the strongest molecular bands at about 770, 1066, 1379, 1425, 1430, 1574, and 1625 cm^{-1} and a broad feature in the range 450−650 cm^{-1} containing distinct peaks at about 515, 595, and 646 cm^{-1}. The absence of the S−H stretching vibration bands at about 2650 cm^{-1} (not shown in the plot) confirmed the cleavage of the S−H bond with the ensuing formation of thiolate structures.

The significant vibrations for 2-NT in the region 200−1000 cm^{-1} are assigned to the in-plane deformation of the ring with C−S contribution, and the two in-plane ring breathing modes, respectively, the strongest band being at about 765 cm^{-1} (in-plane bending mode).[60] Other relevant bands due to in-plane vibrational frequencies appear at 1080 cm^{-1} (C−H bending) and at 1378, 1430, 1567, and 1620 cm^{-1} (ring stretching modes). The slight decrease in the band positions with respect to the unsupported 2-NT confirmed the interaction between the adsorbed species and the support. It can be noted that the relative intensities of the various vibrational modes remained fairly constant with aging time (Figure 5c, blue, green, and black curves), whereas the broad feature in the range 450−650 cm^{-1} (not shown) had a marked increase in intensity indicating copper surface oxidation.

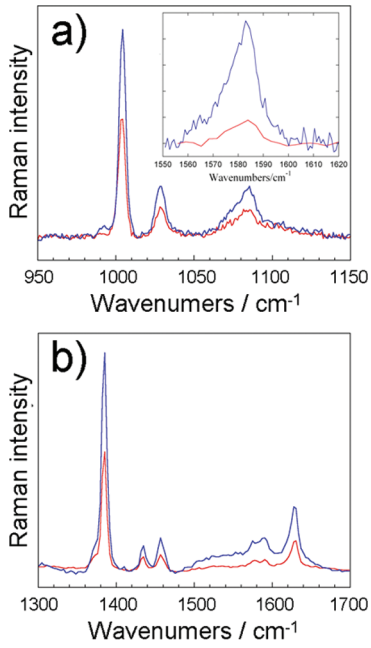

Figure 6. Raman spectra of (a) BT in the region 950−1150 cm^{-1} (1550−1620 cm^{-1} in the inset) and (b) 2-NT in the region 1300−1700 cm^{-1} on Cu detected on the same sample spot as a function of aging time: (red line) freshly prepared sample; (blue line) after 24 h aging.

Changes in relative intensity of the C═C ring stretching modes at 1567, 1580, and 1621 cm^{-1} observed in SERS with respect to 2-NT have been taken to assess the molecule orientation at the surface.[60] In fact the C═C stretching mode normal to the surface results in a band at about 1621 cm^{-1}, whereas a mode parallel to the surface gives a band at 1567 cm^{-1}.

The decrease in intensity of the mode at about 1621 cm^{-1} after 72 and 170 h and the broadening of the bands suggested an evolution toward less ordered structures, with some of them lying almost parallel to the surface. However, as for BT samples, Raman spectra obtained on selected surface spots of freshly prepared and 24 h aged 2-NT samples showed an increase in absolute intensity (Figure 6b) indicative of more regular surface morphology. It is worth noticing that this evolution of 2-NT Raman spectra is totally consistent with the electrochemical data reported above.

The Raman spectra of 1-UT (Figure 5b) on copper were poorly defined and dominated by the strong feature in the range 400−800 cm^{-1} (not shown in the plot), where the CuO vibration and the ν(C−S) stretching mode occur. In the Raman spectra of alkanethiol monolayers formed from various $CH_3(CH)_nSH$ thiols, usually in SERS configuration, the most prominent bands occur in the 600−750 cm^{-1} range for the ν(C−S) stretching mode and in the 1000−1100 cm^{-1} range for the ν(C−C) stretching vibrations. The ν(C−H) vibrations, including symmetric and antisymmetric stretching and deformation modes yield complex structures occur in the range 2800−2950 cm^{-1} and 1410−1480 cm^{-1}, respectively. Rocking and wagging (CH_2) modes are in the range 708−905 cm^{-1} and 1270−1370 cm^{-1}, respectively. The ν(C−S) region can provide conformational information about C−C bonds adjacent to the C−S bond. In the range 600−750 cm^{-1} adsorbed alkanethiol molecules give two bands[57] assigned to gauche (G) conformation, $\nu(C-S)_G$, at about 655 cm^{-1} and to

dx.doi.org/10.1021/jp210041v | J. Phys. Chem. C 2012, 116, 4628−4636

trans (T) conformation, $\nu(C-S)_T$, at about 730 cm^{-1}. Comparing their intensities with those for the respective molecules in the liquid phase, the (G) conformation indicates disorder and therefore it is absent in the solid phase. In the spectrum of as-prepared 1-UT (Figure 6b, red curve), the prominent band at about 725 cm^{-1} can be attributed to $\nu(C-S)_T$ vibration, indicating that the adsorbed molecules were preferentially in the trans conformation. This band strongly decreased in intensity with aging time of 24 h (Figure 6B, blue curve), and it became almost undetectable after 72 h.

The sharp mode at about 895, 1065, and 1120 cm^{-1}, due to CH_2 rocking and C−C stretching vibrations, and at about 1375 and 1440 cm^{-1}, ascribed to C−H deformation modes, recorded on the UT fresh sample, also were strongly attenuated after an aging time of 24 h. All these findings suggest that the adsorption of 1-UT is labile, yielding structures becoming highly disordered after a short time, although the initial data revealed ordered structures.

DCA Measurements. The surface free energy change of copper surface reacted with hydrocarbon thiols can be easily studied by water wetting experiments. The clean copper surface resulted highly wettable, with $\vartheta_{adv} = 44°$ and $\vartheta_{rec} = 11°$. Upon reaction with the various thiols, the noticeable increase recorded for advancing angles confirmed the formation of the hydrophobic SAMs. In Figure 7, the mean value ($n \geq 3$) of

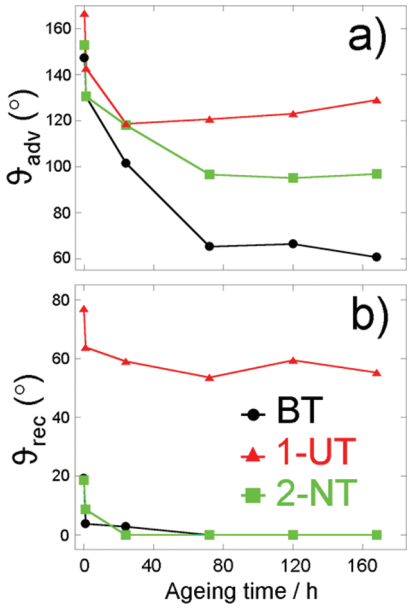

Figure 7. Evolution of (a) advancing contact angle and (b) receding contact angle in ultra pure water as a function of the aging time for various samples: −●− BT, −▲− 1-UT, and −■− 2-NT.

advancing and receding contact angle variation of SAMs as a function of aging time in acidic medium is reported. The results obtained with freshly prepared samples were rather far from those reported in literature for similar systems on gold.[61,62] In particular, we observed a very large hysteresis in all the samples, when compared to that reported in those work. In our opinion, this is probably related to a large difference in roughness between the respective substrates. A significantly high roughness can strongly affect both the values of advancing and reciding angle, leading to a noticeable increase of the hysteresis.[63] As already observed in XPS analysis, the increase of the adsorption time from 2 h, used in a previous research,[32] to 24 h in this work, brought about a better 2-NT coverage of the copper surface, whose initial ϑ_{adv} increases from 102° to 153°. It is interesting to observe that the alkylic 1-UT sample showed the higher advancing and, especially, receding contact angle and the lower hysteresis ($\Delta\vartheta = \vartheta_{adv} - \vartheta_{rec}$). This behavior can be related to the higher hydrophobic character of the alkylic chains with respect to the relatively polar aromatic moiety and to the larger thickness of the 1-UT film. Similar results were already found by Ulman et al., who compared the wettability of aromatic and alkylic SAMs on gold.[62]

The dwelling process of the samples in diluted H_2SO_4 solution demonstrated that the wetting properties variation depended on the copper surface adlayer. The 1-UT-coated sample showed the minor changes and maintained its hydrophobicity, the ϑ_{adv} leveling off after 24 h at a value of 120°. The relatively small ϑ_{adv} and ϑ_{rec} decrease can be assigned to the serious layer damage, partially compensated by the alkylic chain collapse on the copper surface. Nevertheless, the conservation of a highly hydrophobic character confirms that the molecules did not desorb from the surface during the exposure to the electrolyte. On the other hand, an unexpected dramatic increase of wettability has been recorded for BT sample, which, after an aging period of 72 h, reached the lowest advancing contact angle ($\vartheta_{adv} \sim 60°$) and a complete water wettability in the receding cycle ($\vartheta_{rec} = 0$). An intermediate behavior was observed for the advancing results of 2-NT SAM and, as for BT, $\vartheta_{rec} = 0$ after about 24 h. Considering the results of all the other experiments, these unexpected results cannot be ascribed neither to a desorption of the aromatic films nor to a loss in their structural order. A possible explanation for the observed phenomena may be related to the different ability of the chemisorbed molecules to interact with water. In fact it is well-known that the aromatic molecules, besides establishing weak van der Waals interaction, can act as a hydrogen bond acceptor for two water molecules, with their O−H bonds oriented toward the two faces of the aromatic ring.[64] This process could bring about the adsorption of water molecules on SAM surface and, thus, the overall sample wettability increase. Nevertheless, such explanation should be considered currently at the stage of hypothesis, and it is not possible to exclude other factors affecting the great variation of the recorded contact angles.

DISCUSSION

The body of information provided by the multitechnique approach adopted unambiguously demonstrated that SAMs constituted by simple aromatic thiols provide a more efficient and a more durable protection of copper surfaces in acidic environments with respect to alkylic thiols, in spite of their lower thickness. The experiments performed on freshly prepared samples excluded this result from being related to an initial deficiency of 1-UT adlayers which, before the aging in H_2SO_4, exhibited full surface coverage, good structural order, and the best passivating behavior. The two electrochemical techniques clearly showed that the protective properties of the aromatic layers improved after exposure to acidic solutions, surpassing those of 1-UT. XPS measurements established that such improvement occurred without significant changes in layers composition, suggesting that in such conditions aromatic SAMs undergo a structural reorganization leading to a reduction of disordered domains. The increased intensity of the Raman bands of BT and 2-NT aged for 24 h provided confirmation that the observed protection improvement is

dx.doi.org/10.1021/jp210041v | J. Phys. Chem. C 2012, 116, 4628−4636

actually related to an enhancement of the structural order of the layer. The reason for the increasing passivation of aromatic SAMs is also suggested by the trend of the OCP: the negative shift of the corrosion potential implies a higher overpotential in the cathodic corrosion reaction, i.e., the organic monolayer gradually becomes more effective in slowing down oxygen diffusion toward the metal surface. This is coherent with a reduction of structural defects in the aromatic layers during the first hours of aging.

The reasons of such structural reorganization are still unclear. An interesting finding in this regard is represented by the sequence of DCA data taken at different aging times, highlighting an unexpected increase in the wettability of the aromatic SAMs and especially for BT samples. Since, as discussed in the previous section, these results cannot be related to a degradation of the aromatic films, we believe that they could be due to the establishment of a hydrogen-π interaction between the water molecules of the solvent and the aromatic rings of the layers. In fact, although water and benzene are immiscible, the existence of relatively strong interaction between water and conjugated systems, which can lead even to the formation of molecular cluster,[65] has been exhaustively demonstrated both theoretically[66−68] and experimentally.[69,70] The binding energy between a benzene ring and a water molecule was estimated to be −3.9 kcal mol^{-1}, i.e., only 20% weaker than the water−water interaction energy.[71] Literature reports also suggest that such interaction could be the cause of the rearrangement observed in the aromatic samples following the aging. In fact, Monte Carlo simulations on liquid water−benzene systems have shown that the interfacial benzene molecules assume a preferential orientation,[72] and π-hydrogen interactions were observed even between benzene and ice surfaces,[73] where the mobility of water molecules is dramatically limited. Similarly, in our opinion, the contact with the acidic solution might promote a small but significant rearrangement of the molecules driven by the optimization of benzene ring/water interactions, allowing the aromatic layers to heal some structural defects and to keep an ordered structure for a longer time. This ability, together with the higher strength of the S−C bond, would considerably slow down the deterioration process, conferring to aromatic SAMs their remarkable durability. A partial confirmation of the above is provided by the similar behavior observed for the same thiols adsorbed on a polycrystalline gold surface and aged in ultrapure water (still unpublished results of our laboratory). In any case, further experiments will be necessarily required to confirm this hypothesis.

In all the experiments, 2-NT always maintained an intermediate behavior, showing improved performance like BT in the first 48−72 h, and then suddenly undergoing a very rapid breakdown. This is probably related to the presence of a small amount of sulfonate and physisorbed materials already in the freshly prepared samples, as detected by XPS, which could facilitate the formation of pinhole defects, affecting the performance and the stability of the protective layer. Nevertheless, considering the relatively large size of 2-NT molecules and its rigid structure, the hypothesis of a slight deficiency in the surface coverage, little enough to be undetectable by S/Cu atomic ratio, cannot be definitively excluded.

CONCLUSIONS

Adsorbed SAMs of BT, 2-NT and 1-UT on a polycrystalline copper surface, and their evolution in a strongly acidic aqueous solution have been thoroughly investigated by complementary techniques, allowing us to check the layer structure, composition and ability to inhibit the copper corrosion process, as a function of the aging time. All the experiments coherently agree, indicating for the aromatic SAMs, and especially for BT samples, a higher durability in spite of their lower thickness, thanks to a noticeable increase in their protective properties observed during the first hours of aging. Our results strongly suggest this improvement to be related to a structural reorganization of the monolayer, leading to a minimization of disordered domains. This process could be driven by the establishment of π-hydrogen interactions between aromatic rings and water molecules, but further experiments will be required to confirm this hypothesis. The observation of this enhancement in the structural order and in the stability of the aromatic layers when in contact with aqueous solutions could represent an important step toward a broader employment of thiol SAMs, on copper as well as on other substrates, which is currently limited by the relatively rapid degradation of the alkylic layer.

ASSOCIATED CONTENT

Supporting Information

EIS spectra and core fit of the XPS S 2p region of the various samples at different aging time, together with core fit of XPS C1s region, CuLMM Auger spectra of as prepared samples, and Cu2p XP spectra of as prepared samples. This material is available free of charge via the Internet at http://pubs.acs.org

AUTHOR INFORMATION

Corresponding Author

*E-mail address: Supercap81@libero.it.

Notes

The authors declare no competing financial interest.

ACKNOWLEDGMENTS

We wish to thank Prof. R. Zanoni and his group for helpful assistance in using the XPS facility. The financial support by "Sapienza" University is gratefully acknowledged.

REFERENCES

(1) Jones, D. A. *Principles and Prevention of Corrosion*, 2nd ed.; Prentice Hall: Upper Saddle River, NJ, 1996.
(2) Laibinis, P. E.; Whitesides, G. M.; Allara, D. L.; Tao, Y.-T.; Parikh, A. N.; Nuzzo, R. G. *J. Am. Chem. Soc.* **1991**, *113*, 7152.
(3) Laibinis, P. E.; Whitesides, G. M. *J. Am. Chem. Soc.* **1992**, *114*, 9022.
(4) Scherer, J.; Vogt, M. R.; Magnussen, O. M.; Behm, R. J. *Langmuir* **1997**, *13*, 7045.
(5) Ma, H. Y.; Yang, C.; Chen, S. H.; Jiao, Y. L.; Huang, S. X.; Li, D. G.; Luo, J. L. *Electrochim. Acta* **2003**, *48*, 4277.
(6) Li, G.; Ma, H.; Jiao, Y.; Chen, S. *J. Serb.Chem. Soc.* **2004**, *69*, 791.
(7) Sinapi, F.; Lejeune, I.; Delhalle, J.; Mekhalif, Z. *Electrochim. Acta* **2007**, *52*, 5182.
(8) Mekhalif, Z.; Sinapi, F.; Laffineur, F.; Delhalle, J. *J. Electron Spectrosc. Relat. Phenom.* **2001**, *121*, 149.
(9) Sinapi, F.; Julien, S.; Auguste, D.; Hevesi, L.; Delhalle, J.; Mekhalif, Z. *Electrochim. Acta* **2008**, *53*, 4228.
(10) Feng, Y.; Teo, W.-K.; Siow, K.-S.; Gao, Z.; Tan, K.-L.; Hsieh, A.-K. *J. Electrochem. Soc.* **1997**, *144*, 55.
(11) Metikoš-Huković, M.; Babić, R.; Petrović, Ž.; Posavec, D. *J. Electrochem. Soc.* **2007**, *154*, C138−C143.
(12) Petrović, Ž.; Metikoš-Huković, M.; Babić, R. *Prog. Org. Coat.* **2008**, *61*, 1.

(13) Yamamoto, Y.; Nishiara, H.; Aramaki, K. *J. Electrochem. Soc.* **1993**, *140*, 436.
(14) Ishibashi, M.; Itoh, M.; Nishihara, H.; Aramaki, K. *Electrochim. Acta* **1996**, *41*, 241.
(15) Jennings, G. K.; Munro, J. C.; Laibinis, P. E. *Adv. Mater.* **1999**, *11*, 1000.
(16) Ma, H. Y.; Yang, C.; Yin, B. S.; Li, G. Y.; Chen, S. H.; Luo, J. L. *Appl. Surf. Sci.* **2003**, *218*, 143.
(17) Wang, P.; Yang, C.; Wu, B.; Huang, N.; Li, J. *Electrochim. Acta* **2010**, *55*, 878.
(18) Loepp, G.; Vollmer, S.; Witte, G.; Wöll, Ch. *Langmuir* **1999**, *15*, 3767.
(19) Vollmer, S.; Fouquet, P.; Witte, G.; Boas, Ch.; Kunat, M.; Burghaus, U.; Wöll, Ch. *Surf. Sci.* **2000**, *462*, 135.
(20) Tan, Y. S.; Srinivasan, M. P.; Pehkonen, S. O.; Chooi, S. Y. M. *J. Vac. Sci. Technol., A* **2004**, *22*, 1917.
(21) Jennings, G. K.; Munro, J. C.; Yong, T.-H.; Laibinis, P. E. *Langmuir* **1998**, *14*, 6130.
(22) Itoh, M.; Nishiara, H.; Aramaki, K. *J. Electrochem. Soc.* **1994**, *141*, 2018.
(23) Itoh, M.; Nishiara, H.; Aramaki, K. *J. Electrochem. Soc.* **1995**, *142*, 3696.
(24) Itoh, M.; Nishiara, H.; Aramaki, K. *J. Electrochem. Soc.* **1995**, *142*, 1839.
(25) Haneda, R.; Nishiara, H.; Aramaki, K. *J. Electrochem. Soc.* **1997**, *144*, 1215.
(26) Haneda, R.; Aramaki, K. *J. Electrochem. Soc.* **1998**, *145*, 2786.
(27) Haneda, R.; Aramaki, K. *J. Electrochem. Soc.* **1998**, *145*, 1856.
(28) Jennings, G. K.; Yong, T.-H.; Munro, J. C.; Laibinis, P. E. *J. Am. Chem. Soc.* **2003**, *125*, 2950.
(29) Srivastava, P.; Chapman, W. G.; Laibinis, P. E. *Langmuir* **2009**, *25*, 2689.
(30) Whelan, C. M.; Kinsella, M.; Carbonell, L.; Ho, H. M.; Maex, K. *Microelectron. Eng.* **2003**, *70*, 551.
(31) Tan, Y. S.; Srinivasan, M. P.; Pehkonen, S. O.; Chooi, S. Y. M. *Corros. Sci.* **2006**, *48*, 840.
(32) Caprioli, F.; Beccari, M.; Martinelli, A.; Di Castro, V.; Decker, F. *Phys. Chem. Chem. Phys.* **2009**, *11*, 11624.
(33) Caprioli, F.; Decker, F.; Marrani, A. G.; Beccari, M.; Di Castro, V. *Phys. Chem. Chem. Phys.* **2010**, *12*, 9230.
(34) Zamborini, F. P.; Campbell, J. K.; Crooks, R. M. *Langmuir* **1998**, *14*, 640.
(35) Käfer, D.; Bashir, A.; Witte, G. *J. Phys. Chem. C* **2007**, *111*, 10546.
(36) Frey, S.; Stadler, V.; Heister, K.; Eck, W.; Zharnikov, M.; Grunze, M.; Zeysing, B.; Terfort, A. *Langmuir* **2001**, *17*, 2408.
(37) Schmidt, C.; Götzen, J.; Witte, G. *Langmuir* **2011**, *27*, 1025.
(38) Beccari, M.; Kanjilal, A.; Betti, M. G.; Mariani, C.; Floreano, L.; Cossaro, A.; Di Castro, V. *J. Electron Spectrosc. Relat. Phenom.* **2009**, *172*, 74.
(39) *CRC Handbook of Chemistry and Physics*, 91st ed.; CRC Press: Boca Raton, FL, 2011; Chapter 9 (Internet version).
(40) Caprioli, F.; Decker, F.; Di Castro, V. *J. Electroanal. Chem.* **2011**, *657*, 192.
(41) Vericat, C.; Vela, M. E.; Benitez, G.; Carro, P.; Salvarezza, R. C. *Chem. Soc. Rev.* **2010**, *39*, 1805.
(42) Scofield, J. H. *J. Electron Spectrosc. Relat. Phenom.* **1976**, *8*, 129.
(43) Bobour, E.; Lennox, R. B. *J. Phys. Chem. B* **2000**, *104*, 9004.
(44) Li, D.; Yu, X.; Dong, Y. *Appl. Surf. Sci.* **2007**, *253*, 4182.
(45) Abelev, E.; Starosvetsky, D.; Ein-Eli, Y. *Langmuir* **2001**, *23*, 11281.
(46) Castner, D. G.; Hinds, K.; Grainger, D. W. *Langmuir* **1996**, *12*, 5083.
(47) Lindberg, B. J.; Hamrin, K.; Johansson, G.; Gelius, U.; Fahlman, A.; Nordling, C.; Siegbahn, K. *Phys. Scr.* **1970**, *1*, 286.
(48) Boccia, A.; Lanzillotto, V.; Di Castro, V.; Zanoni, R.; Pescatori, L.; Arduini, A.; Secchi, A. *Phys. Chem. Chem. Phys.* **2011**, *13*, 4452.
(49) Zharnikov, M.; Grunze, M. *J. Phys.: Condens. Matter* **2001**, *13*, 11333.
(50) Kühnle, A.; Vollmer, S.; Linderoth, T. R.; Witte, G.; Wöll, C.; Besenbacher, F. *Langmuir* **2002**, *18*, 5558.
(51) Contini, G.; Laajalehto, K.; Suoninen, E.; Marabini, M. *J. Electron Spectrosc. Relat. Phenom.* **1995**, *171*, 234.
(52) Zhao, J.; Xu, D.; Zhang, K.; Cheng, X. *J. Mol. Struct.: THEOCHEM* **2009**, *909*, 9.
(53) Luo, Y. R. *Handbook of Bond Dissociation Energies in Organic Compounds*; CRC Press: Boca Raton, FL, 2003.
(54) Kudelski, A. *Vib. Spectrosc.* **2005**, *39*, 200.
(55) Li, S.; Wu, D.; Xu, X.; Gu, R. *J. Raman Spectrosc.* **2007**, *38*, 1436.
(56) Carron, K. T.; Hurley, L. G. *J. Phys. Chem.* **1991**, *95*, 9979.
(57) Bryant, M. A.; Pemberton, J. E. *J. Am. Chem. Soc.* **1991**, *113*, 8284.
(58) Szafranski, C. A.; Tanner, W.; Laibinis, P. E.; Garrell, R. L. *Langmuir* **1998**, *14*, 3570.
(59) Yua, T.; Zhaoa, X.; Shena, Z. X.; Wub, Y. H.; Sud, W. H. *J. Cryst. Growth* **2004**, *268*, 590.
(60) Alvarez-Puebla, R. A.; Dos Santos, D. S. Jr.; Aroca, R. F. *Analyst (Cambridge, U. K.)* **2004**, *129*, 1251.
(61) Barriet, D.; Yam, C. M.; Shmakova, O. E.; Jamison, A. C.; Lee, T. R. *Langmuir* **2007**, *23*, 8866.
(62) Kang, J. F.; Ulman, A.; Liao, S.; Jordan, R.; Yang, G.; Liu, G.-Y. *Langmuir* **2001**, *17*, 95.
(63) Johnson, R. E.; Dettre, R. H. *Adv. Chem. Ser.* **1963**, *43*, 112.
(64) Graziano, G.; Lee, B. *J. Phys. Chem. B* **2001**, *105*, 10367.
(65) Kim, K. S.; Tarakeshwar, P.; Lee, J. Y. *Chem. Rev.* **2000**, *100*, 4145.
(66) Karlström, G.; Linse, P.; Wallquist, A.; Jönsson, B. *J. Am. Chem. Soc.* **1983**, *105*, 3777.
(67) Suzuki, S.; Green, P. G.; Bumgamer, R. E.; Dasgupta, S.; Goddard, W. A. III; Blake, G. A. *Science* **1992**, *275*, 942.
(68) Fredericks, S. Y.; Jordan, K. D.; Zwier, T. S. *J. Phys. Chem.* **1996**, *100*, 7810.
(69) Gotch, A. J.; Zwier, T. S. *J. Chem. Phys.* **1992**, *96*, 3388.
(70) Pribble, R. N.; Garret, A. W.; Haber, K.; Zwier, T. S. *J. Chem. Phys.* **1995**, *103*, 531.
(71) Feller, D. *J. Phys. Chem. A* **1999**, *103*, 7558.
(72) Kereszturi, A.; Jedlovszky, P. *J. Phys. Chem. B* **2005**, *109*, 16782.
(73) Silva, S. C.; Devlin, J. P. *J. Phys. Chem.* **1994**, *98*, 10847.